Development and Testing of a Surface Flux and Planetary Boundary Layer Model for Application in Mesoscale Models

JONATHAN E. PLEIM*

Atmospheric Sciences Modeling Division, Air Resources Laboratory, National Oceanic and Atmospheric Administration, Research Triangle Park, North Carolina

AIJUN XIU

Environmental Programs, MCNC, North Carolina Supercomputing Center, Research Triangle Park, North Carolina

(Manuscript received 1 November 1993, in final form 24 February 1994)

ABSTRACT

Although the development of soil, vegetation, and atmosphere interaction models has been driven primarily by the need for accurate simulations of long-term energy and moisture budgets in global climate models, the importance of these processes at smaller scales for short-term numerical weather prediction and air quality studies is becoming more appreciated. Planetary boundary layer (PBL) development is highly dependent on the partitioning of the available net radiation into sensible and latent heat fluxes. Therefore, adequate treatment of surface properties such as soil moisture and vegetation characteristics is essential for accurate simulation of PBL development, convective and low-level cloud processes, and the temperature and humidity of boundary layer air.

In this paper, the development of a simple coupled surface and PBL model, which is planned for incorporation into the Pennsylvania State University–National Center for Atmospheric Research Mesoscale Model (MM4/5), is described. The soil–vegetation model is based on a simple force–restore algorithm with explicit soil moisture and evapotranspiration. The PBL model is a hybrid of nonlocal closure for convective conditions and eddy diffusion for all other conditions. A one-dimensional version of the model has been applied to several case studies from field experiments in both dry desert-like conditions (Wangara) and moist vegetated conditions (First International Satellite Land Surface Climatology Project Field Experiment) to demonstrate the model's ability to realistically simulate surface fluxes as well as PBL development. This new surface–PBL model is currently being incorporated into the MM4–MM5 system.

1. Introduction

There has been increasing realization recently that realistic simulation of surface fluxes is extremely important for 3D mesoscale modeling. Particularly, the evolution and maximum depth of the planetary boundary layer (PBL) is highly dependent on the partitioning of the available net radiation into sensible and latent heat fluxes. Clearly, this partitioning also has profound importance to low-level cloud formation (Wetzel and Argentini 1990). In addition, mesoscale fluxes of heat due to secondary circulations caused by spatially varying land use have been shown to be of the same order of magnitude as turbulent fluxes (Pielke et al. 1991). Therefore, adequate treatment of surface properties such as soil moisture and vegetation characteristics are essential for accurate simulations of PBL development and cloud coverage, both of which are key factors influencing atmospheric chemistry and air quality.

Several models have been developed in recent years for the simulation of surface–vegetation–atmosphere exchange in meteorological models (Sellers et al. 1986; Dickinson et al. 1986; Wetzel and Chang 1987; Noilhan and Planton 1989). Most of these models evolved from the methods presented by Deardorff (1978), who described a force–restore algorithm for both surface temperature and near-surface soil moisture. The key processes that need to be represented in these models include short- and longwave radiation, turbulent surface fluxes of heat and moisture, evapotranspiration, and heat and moisture fluxes within the soil. The sensitivity of these models to various vegetative and soil characteristics have been investigated by Wilson et al. (1987) and Mihailovic et al. (1992). A key concern related to the use of these models, which are essentially 1D and very local in scale, in mesoscale or larger-scale grid models is the effects of subgrid heterogeneity of land

* On assignment to the Atmospheric Research and Exposure Assessment Laboratory, U.S. Environmental Protection Agency, Research Triangle Park, North Carolina.

Corresponding author address: Dr. Jonathan E. Pleim, U.S. EPA, MD-80, Research Triangle Park, NC 27711.

surface characteristics (primarily vegetation and soil type). One aspect of this issue, which was studied by Wetzel and Chang (1988), is the nonlinearity of horizontal averaging over varying surface conditions within each model grid cell. Another aspect of this issue, which was described by Avissar and Pielke (1989), is the occurrence of subgrid circulations resulting from contrasting surface conditions.

For many years the Pennsylvania State University–National Center for Atmospheric Research Mesoscale Model Version 4 (MM4) (Anthes et al. 1987) has been used as the meteorological driver for the Regional Acid Deposition Model (RADM) (Chang et al. 1987). However, the capability of this model for accurate characterization of the PBL, particularly the daytime PBL height, has been found to be somewhat lacking. For example, a model evaluation study of the MM4–RADM system conducted during the summer of 1988, which included aircraft measurements over a large area of the eastern United States, showed consistently underpredicted PBL heights (Pleim and Ching 1993). Since the summer of 1988 was extraordinarily dry in the eastern United States, the underprediction of PBL heights reflects the model's insensitivity to surface moisture conditions.

The current MM4 system uses a force–restore ground temperature algorithm in the manner of Deardorff (1978). This scheme, however, does not include the prognostic simulation of soil moisture but instead uses a moisture availability factor to specify the effective soil moisture available for evaporation. A drawback of this approach is that these moisture availability factors are functions of land use category only and therefore have no ability to respond to changes in soil moisture conditions. Therefore, MM4 simulations of PBL height, surface temperature, PBL temperature and humidity, and low-level cloud development may be significantly unrealistic whenever soil moisture conditions differ from the assumed moisture availability. Since RADM simulations of chemical concentrations depend enormously on PBL height, we decided to embark on an effort to upgrade this part of the MM4 system.

In this paper, we describe the development of a simple surface–PBL model for eventual inclusion into the MM4. The model consists of a land surface model for the prognostic simulation of soil moisture and soil temperature, a PBL model for the simulation of vertical turbulent transport of heat, moisture, and momentum, a flux-profile algorithm that couples the surface with the atmosphere through the surface fluxes, and a simple surface radiation model. The land surface portion of the model is based on a model developed by Noilhan and Planton (1989). The PBL module and flux-profile relationships are the same as currently used in the latest version of RADM. The PBL model is a hybrid of nonlocal closure, for convective conditions, and eddy diffusion. A preliminary version of the model, initially in 1D form, is applied to two field studies for comparison, where one case was in a dry sparsely vegetated desert (Wangara) and the other in a rather moist long grass prairie [First ISLSCP (International Satellite Land Surface Climatology Project) Field Experiment (FIFE)]. Note that these case studies represent the initial testing of a model that is still under development (e.g., the effects of condensation and clouds are yet to be included). Last, a test is made of the sensitivity of PBL height and surface temperature to soil moisture initialization in order to demonstrate the range of errors likely to result from the neglect of soil moisture variation. The next stage of this effort will be to incorporate the surface–PBL model described here into the MM4–MM5 system. This 3D model will then be extensively tested for a variety of conditions and seasons to test the model's ability to realistically respond to heterogeneous vegetation and soil conditions as well as time-varying soil hydrology. These are all capabilities absent from the current version of MM4/5.

2. Model description

a. Soil–vegetation model

The soil–vegetation model used in this study was developed specifically for use in mesoscale meteorology models. It has been extensively documented and tested first in a 1D prototype (Noilhan and Planton 1989; Jacquemin and Noilhan 1990) and more recently in a comprehensive 3D meso-β-scale meteorology model as described in a series of three papers (Bougeault et al. 1991a; Bougeault et al. 1991b; Noilhan et al. 1991). In both cases, model results were compared to extensive field measurement data from the HAPEX–MOBILHY experiment (André et al. 1986), which included both cropland and forest. The model is designed to simulate the essential processes involved in surface–atmosphere interactions with the fewest parameters and complexities. For example, one temperature is used for both vegetation and the soil surface unlike some canopy resolving models (Sellers et al. 1986; Dickinson et al. 1986), which simulate ground and canopy temperatures separately. Furthermore, compared to some of the more complex models, the additional data requirements are minimal. Specifically, incorporation of this model into the MM4 would require the addition of only soil texture classification, leaf area index (LAI), minimal stomatal resistance, and fractional vegetative cover to the model input database. Note that roughness length is also needed by this scheme but MM4 already uses this parameter. Therefore, the combination of simplicity, minimal data requirements, and the model's proven performance over a variety of land use conditions made it a logical choice for use in the MM4 system.

The soil–vegetation model includes prognostic equations for both soil and vegetation temperature and soil moisture using a two-layer force–restore algorithm. The driving force for the prognostic simulation of sur-

face temperature is the surface energy budget that includes net radiation, sensible heat flux, latent heat flux, and heat flux into the ground. Similarly, the surface soil moisture is driven by the surface moisture budget, which includes precipitation and dew formation, direct evaporation from the ground and canopy, evapotranspiration, and moisture flux within the soil. Transpiration through vegetation directly from the lower soil layer (root zone) is modeled via a stomatal resistance analog algorithm. The details of the land-surface model can be found in both Noilhan and Planton (1989) and Jacquemin and Noilhan (1990). Our version of the model was coded directly from these papers. The model is based on the following set of five partial differential equations:

$$\frac{\partial T_s}{\partial t} = C_T(R_n - H - LE) - \frac{2\pi}{\tau}(T_s - T_2) \quad (1)$$

$$\frac{\partial T_2}{\partial t} = \frac{1}{\tau}(T_s - T_2) \quad (2)$$

$$\frac{\partial w_g}{\partial t} = \frac{C_1}{\rho_w d_1}(P_g - E_g) - \frac{C_2}{\tau}(w_g - w_{geq}) \quad (3)$$

$$\frac{\partial w_2}{\partial t} = \frac{1}{\rho_w d_2}(P_g - E_g - E_{tr}) \quad (4)$$

$$\frac{\partial W_r}{\partial t} = \text{veg}P - E_r, \quad (5)$$

where T_s is the soil surface temperature (nominally 1 cm) and T_2 is the average temperature of the lower layer (usually 1 m), which acts as a slowly varying heat reservoir. Here w_g is the volumetric soil moisture in the top 1 cm (d_1) and w_2 is the average volumetric soil moisture down to about 1 m (d_2). Here W_r is the amount of water in the canopy, which is limited to $W_{r\max} = h$ vegLAI where $h = 0.2$ mm, and veg is the fractional coverage of vegetation; P is precipitation rate and P_g is the precipitation rate reaching the ground; and E_g and E_{tr} are the evaporation rates from the ground and by transpiration, respectively. Note that volumetric soil moisture (w_g and w_2) is limited to the soil saturation point. If the net change in soil moisture (precipitation − evaporation) would result in soil moisture greater than saturation, the excess is assumed to runoff.

Equation (1) shows that local changes in soil surface temperature result from the residual of the surface energy balance among net radiation R_n, surface heat flux H, latent heat flux LE, and soil heat flux, which is parameterized as a restoring force on the soil temperature back toward the diurnal average (τ is the time constant—1 day). The coefficient C_T in Eq. (1), which represents the inverse of the bulk heat capacity of the surface and vegetation, is a function of the deeper layer soil moisture w_2 as shown in Noilhan and Planton (1989). Expressions for the soil moisture coefficients C_1, C_2, and for w_{geq}, which is essentially w_2 modified to account for gravity, are given in the appendix of Jacquemin and Noilhan (1990). These are expressed in terms of soil parameters, such as field capacity, wilting point, saturation, and various thermal and hydraulic properties of the soil, which are specified according to the 11 soil types of the U.S. Department of Agriculture (USDA) textural classification (Clapp and Hornberger 1978). Therefore, the only soil data required for this model is the soil texture type. In our version of this model, Eqs. (1)–(5) are integrated using a semi-implicit Crank–Nicolson technique.

A notable variation of our model from the work of Noilhan and Planton (1989) is in the coefficient C_T (inverse of the bulk heat capacity), which they define as the harmonic average of the value for soil and the value for vegetation weighted by the vegetative fractional coverage. Their rationale is that for areas completely shielded by vegetation the relevant surface temperature for computing surface fluxes is that of the vegetation and not the ground. The problem with this approach is that the value they use for the heat capacity of vegetation is practically negligible leading to virtually no heat storage at the surface. This goes against some observational evidence that even in highly vegetated areas, such as grasslands, there is a significant soil heat flux and lag to morning surface heating. For example, the daytime (8 h centered on local noon) soil flux averaged over all sites and measurement days during the 1987 FIFE, where the ground was essentially completely covered by tall grass, was about 50 W m^{-2}, which is 13% of the averaged net radiation (Smith et al. 1992b). Therefore, for these case studies, rather than using the weighted average of soil and vegetation heat capacities, we simply used the soil heat capacity regardless of vegetative cover.

Other investigators (Argentini et al. 1992; Wetzel and Chang 1988) have parameterized the heat capacity of vegetation according to the amount of liquid water contained within the plants as well as any water in the canopy from rain or dew. Thus, the heat capacity of biomass in their models is simply $(b_m + W_r)C_w$, where b_m is the water equivalent biomass, W_r is dew and rainwater in the canopy, and C_w is the heat capacity of water. In areas of dense vegetation, such as forests or agricultural crops the biomass heat capacity can significantly delay surface heating in the morning. However, for the cases studies presented here the heat capacity of the soil was probably much greater than the biomass heat capacity.

b. Planetary boundary layer model

The PBL model is a hybrid of a simple nonlocal closure scheme used during conditions of free convection and an eddy diffusion scheme for all other conditions. The criterion currently used to define free convective conditions is $h/L < -3$, where h is the height

of the PBL and L is the Monin–Obukhov length. The nonlocal closure model, referred to as the "asymmetrical convective model" (ACM), is designed to simulate rapid upward transport from the surface layer to all levels within the convective boundary layer (CBL) by rapidly rising buoyant plumes and more gradual downward transport by broad slow compensatory subsidence (Fig. 1). The ACM was developed from the convective model of Blackadar (1978), which is currently used in MM4. The ACM retains the direct nonlocal upward flux of the Blackadar model but replaces the downward return flux with a local layer by layer approach, thereby combining the rapid upward convection of the Blackadar model with diffusion-like subsidence. The ACM has been shown, through comparison to large-eddy simulations, to provide a more realistic simulation of vertical fluxes in the CBL than either the Blackadar model or local eddy diffusion schemes without a significant increase in computational expense (Pleim and Chang 1992).

For all conditions other than free convective a simple eddy diffusion model is used. The eddy diffusivities are based on surface-layer and boundary layer length and velocity scaling in the manner of Holtslag and Nieuwstadt (1986), Troen and Mahrt (1986), and others. The eddy diffusion model is described in the appendix of Pleim and Chang (1992). An important difference between this scheme and the model currently used in the MM4 (Blackadar 1976) is that the eddy diffusivities K_z within the PBL depend on the estimated height of the PBL. PBL height is estimated according to a bulk Richardson number method as suggested by Holtslag et al. (1990). In this scheme, the PBL bulk Richardson number is computed,

$$\mathrm{Ri}_b = \frac{gz\Delta\theta_v}{\overline{\theta_v}[u(z)^2 + v(z)^2]}, \tag{6}$$

where $\Delta\theta_v = \theta_v(z) - \theta_{vs}$ and $\overline{\theta_v} = 0.5[\theta_v(z) + \theta_{vs}]$, at successive heights z above the ground until $\mathrm{Ri}_b \geq \mathrm{Ri}_c$ ($\mathrm{Ri}_c = 0.25$). The top of the PBL is defined as the height at which Ri_b first equals the critical Richardson number.

The governing equations for the PBL in 1D form (horizontal advection neglected) in σ coordinates [$\sigma = (p - p_{\mathrm{top}})(p_{\mathrm{surf}} - p_{\mathrm{top}})^{-1}$ and $p_{\mathrm{top}} = 10$ kPa] where condensation is not considered are

$$\frac{\partial\theta_v}{\partial t} = \frac{\partial(\overline{w'\theta_v'})}{\partial\sigma} \tag{7}$$

$$\frac{\partial q}{\partial t} = \frac{\partial(\overline{w'q'})}{\partial\sigma} \tag{8}$$

$$\frac{\partial U}{\partial t} = -f(V_g - V) - \frac{\partial(\overline{w'u'})}{\partial\sigma} \tag{9}$$

$$\frac{\partial V}{\partial t} = f(U_g - U) - \frac{\partial(\overline{w'v'})}{\partial\sigma}, \tag{10}$$

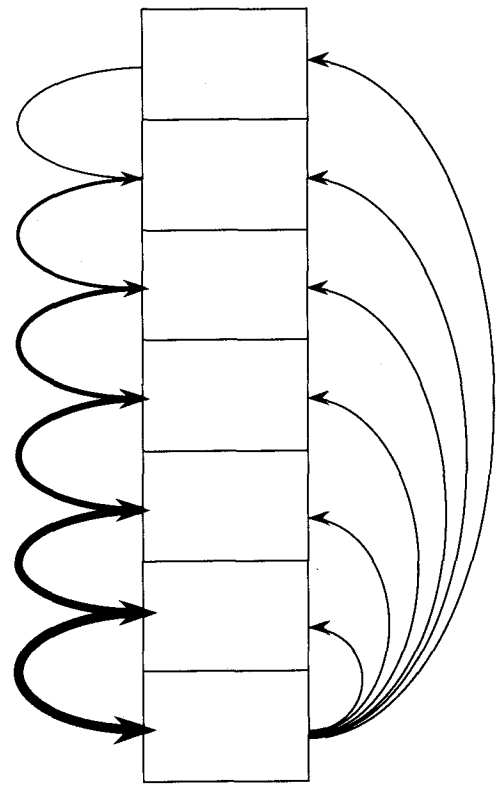

FIG. 1. Schematic representation of mixing in a 1D column of air as simulated by the asymmetrical convective model (ACM). Line thicknesses are proportional to mixing rates.

where θ_v is virtual potential temperature, q is mixing ratio, U and V are the horizontal wind components, and w is the vertical velocity in sigma coordinates ($w = d\sigma/dt$). Primed variables represent turbulent fluctuations from the mean. Here U_g and V_g are the geostrophic wind components, which for the case studies described below were derived from observations and supplied as inputs to the model. For the Wangara case it was possible to resolve the geostrophic winds in time and vertically, thereby incorporating some baroclinic forcing in the simulation. However, this model can perform well only under conditions where horizontal advection and condensation are unimportant. Therefore, the case studies were selected for their lack of clouds and relatively weak horizontal and vertical advection.

The surface model and the PBL model are linked through their respective boundary conditions, namely, the surface fluxes of heat, moisture, and momentum. Heat and momentum fluxes are determined from wind speed and temperature differences between the surface and the lowest atmospheric level using surface layer and the PBL flux-profile relations developed by Byun (1990, 1991) based on Rossby number similarity and profile matching. Humidity fluxes are represented by

the following three parallel pathways: transpiration (E_{tr}),

$$E_{tr} = \rho_a \, \text{veg}(1 - \sigma) \frac{q_{sat}(T_s) - q_a}{r_a + r_s}; \quad (11a)$$

evaporation from wet parts of the canopy (E_r),

$$E_r = \rho_a \, \text{veg}\, \sigma \frac{q_{sat}(T_s) - q_a}{r_a}; \quad (11b)$$

and direct evaporation form the ground (E_g),

$$E_g = \rho_a(1 - \text{veg}) \frac{\text{Hu}\, q_{sat}(T_s) - q_a}{r_a}, \quad (11c)$$

where

$$\text{Hu} = 0.5\left[1 - \cos\left(\pi \frac{w_g}{w_{fc}}\right)\right] \quad (12)$$

and Hu is constrained to 1 if w_g is greater than field capacity (w_{fc}). Veg is the fractional vegetation coverage, and σ is the wet fraction of the canopy. The surface resistance for evapotranspiration is computed as

$$r_s = \frac{r_{s\min}}{\text{LAI} F_1 F_2 F_3 F_4}, \quad (13)$$

where leaf area index (LAI) and minimum stomatal resistance $r_{s\min}$ are specified according to land use classification. The fractional conductances F are functions of solar radiation, root-level soil moisture w_2, air humidity deficit, and ambient air temperature. See Noilhan and Planton (1989) and Jacquemin and Noilhan (1990) for the functional forms of these conductances. The aerodynamic resistance r_a is computed from the difference in virtual potential temperature between the air and the ground and the surface heat flux,

$$r_a = \rho_a C_p \frac{\theta_{va} - \theta_{vg}}{H}. \quad (14a)$$

When heat flux is near zero ($H/\rho_a C_p < 10^{-15}$ K m s^{-1}), during the morning and afternoon transitions, r_a is estimated from neutral surface-layer similarity theory,

$$r_a = \frac{0.74}{u_* k} \ln\left(\frac{z_1}{z_0}\right), \quad (14b)$$

where u_* is the surface friction velocity, k is the von Kármán constant (0.4), z_1 is the center height of the first model level, and z_0 is the roughness length. The surface and PBL models are integrated using operator splitting with a short time step to minimize oscillations of the temperature and humidity in the lowest air layer and surface soil layer that can propagate through the surface fluxes.

c. *Radiation model*

Net radiation flux [R_n in Eq. (1)] at the surface is given by

$$R_n = R_{sw}^{\downarrow}(1 - \alpha)\tau_{sw} - \epsilon_g \sigma T_s^4 + \epsilon_a \sigma T_a^4, \quad (15)$$

where τ_{sw} is the shortwave transmissivity, ϵ_g is the emissivity of the surface, and ϵ_a is the emissivity of the air. Net radiation flux is computed similarly to the MM4 (Anthes et al. 1987) but with some minor improvements. Rather than using a constant surface albedo, as in the MM4, the surface albedo is defined as a function of the solar zenith angle as suggested by the work of Idso et al. (1975), such that the total albedo (α) is

$$\alpha = \alpha_z + \alpha_s, \quad (16)$$

where α_z is a solar zenith angle Z adjustment,

$$\alpha_Z = 0.01[\exp(0.003286 Z^{1.5}) - 1], \quad (17)$$

and α_s is the minimum albedo with a solar zenith angle of zero, which is specified according to surface type. The surface albedo α_s is sometimes specified as a function of soil moisture (McCumber and Pielke 1981), however, this is appropriate only for bare soil.

In MM4 the direct downward solar irradiance reaching a horizontal surface of unit area at the top of the atmosphere ($R_{sw}^{\downarrow}$) is a function of the solar zenith angle only. This quantity, however, also depends on the distance between the earth and the sun such that a more complete formulation is

$$R_{sw}^{\downarrow} = S_0\left(\frac{a^2}{r^2}\right)\cos Z, \quad (18)$$

where a is the average distance from the earth to the sun and r is the distance to the sun as a function of time of year and S_0 is the solar constant. The ratio a^2/r^2 at any specific day of the year can be calculated (from Paltridge and Platt 1976) as

$$\frac{a^2}{r^2} = 1.000110 + 0.034221 \cos d_0 + 0.001280 \sin d_0 + 0.000719 \cos 2d_0 + 0.000077 \sin 2d_0, \quad (19)$$

where $d_0 = 2\pi m/365$ and m is the day number starting with 0 on 1 January and ending 364 on December 31. Note that the effect of the variation of the earth's distance from the sun results in a maximum of 3.3% variation in $R_{sw}^{\downarrow}$.

Shortwave transmissivity for multiple reflection is computed as in the MM4 (Anthes et al. 1987). Clear-air transmissivities for direct and diffuse radiation due to absorption and scattering, as well as backscattering coefficients, are determined as functions of precipitable water and pathlength from a look-up table created from the Carlson and Boland (1978) radiative transfer model. The expressions for transmissivity and the look-up table are given in the MM4 model description (Anthes et al. 1987). Note that the effects of clouds are not included in this study but will be in the next phase of this development when the surface–PBL

model described here is incorporated into the full 3D MM4.

The net longwave radiation at the surface is computed, as shown in Eq. (15), simply as the sum of the upward and downward components. In both cases the blackbody relationship of Stefan–Boltzman is used with the emissivity of the ground ϵ_g set to one and the emissivity of air ϵ_a computed as a function of precipitable water (Monteith 1961),

$$\epsilon_a = 0.725 + 0.17 \log_{10} w_p, \qquad (20)$$

where w_p is the precipitable water computed as the vertical integral of water vapor concentration. Furthermore, the atmospheric temperature T_a used in Eq. (15) is the ambient temperature at the level of the vertical centriod of precipitable water.

3. Modeling results

The initial testing of the combined surface–PBL model is the application of a 1D prototype to the field studies of Wangara (Clarke et al. 1971) and FIFE (Sellers et al. 1992a). The purpose of this effort is to determine the model's ability to simulate real world surface fluxes and PBL characteristics with the eventual goal of improving those aspects of the MM4 for use in air quality modeling. Therefore, the evaluation emphasizes parameters that are most relevant to air quality such as PBL height and surface temperature. However, since these parameters are interdependent with many others, the evaluation of sensible and latent heat fluxes as well as soil moisture are also quite relevant. In addition, moisture fluxes are very important for the moisture loading of the PBL and therefore for cloud development. Clouds have the potential to feedback to surface fluxes of heat and moisture through the obstruction of solar radiation and the moistening of the surface by precipitation. Cloud effects will be studied in the next phase of this work in the context of the 3D MM4.

a. Wangara

The first case study involved a 36-h simulation of days 33 and 34 of the Wangara Boundary Layer Experiment (16 and 17 August 1967) starting at 0900 local time. These particular days have been used quite often as a test case for PBL models (Deardorff 1974; Wyngaard and Coté 1974; Yamada and Mellor 1975; Binkowski 1983) because of clear skies all day and very weak horizontal advection. The site was an arid region of Australia with very sparse vegetation. Therefore, this case does not provide a good test of the soil moisture and evapotranspiration components of the model but is a good test of the PBL and heat flux algorithms. Table 1 lists the surface parameters used in this simulation as well as for the FIFE simulations, which are described in the next section.

TABLE 1. Surface parameters for case studies.

Parameter	Wangara	FIFE	FIFE
Date	16, 17 Aug 1967	11 July 1987	6 June 1987
Soil type	Loam	Silty clay loam	Silty clay loam
z_0 (cm)	0.24	6.5	4.5
LAI	0.1	2.8	1.9
Veg (%)	5	99	99

The model was run with 25 vertical levels up to about 2 km using a σ_p coordinate system. The lowest level was $\Delta\sigma = 0.0025$ or about 20 m thick. The second layer was $\Delta\sigma = 0.0075$ and each layer above was $\Delta\sigma = 0.01$ or about 80 m thick. Temperature and humidity profiles were initialized by interpolation of the 0900 radiosonde measurements and the winds were interpolated from pilot balloon observations at the same time. The soil surface temperature T_s was initialized to the 0900 surface temperature measurement (279 K). Since there was no direct measurement of the deep soil temperature, the initial value had to be inferred from measurements of ground heat flux and surface temperature. At 0800 the ground heat flux was about zero (Clarke et al. 1971) indicating that the deep-layer temperature T_2 was approximately the same as the surface temperature. Therefore T_2 was initialized to the 0800 surface temperature (273 K). Both shallow and deep soil moisture were set to the wilting point as suggested by Clarke et al. (1971) since it had not rained for many days.

Surface geostrophic winds were derived every 3 h from five closely spaced field measurement stations and 14 Bureau of Meteorology stations. In addition, thermal winds in two layers from 0 to 1 km and 1 to 2 km were estimated twice daily (0900 and 2100 LT) from the Bureau of Meteorology synoptic radiosonde network. Hourly estimates of thermal winds were linearly interpolated from the twice daily measurements. Vertical profiles of geostrophic winds were derived from a parabolic fit to the thermal wind data as suggested by Yamada and Mellor (1975). The resulting geostrophic wind estimates as functions of both height and time were supplied to the model as input.

Figure 2 shows both measured and modeled surface fluxes of net radiation, sensible heat, latent heat, and ground heat starting at 0900 LT on day 33 (16 August) and ending at midnight on day 34. Measured net radiation and ground fluxes were reported by Clarke et al. (1971). Sensible heat fluxes were derived according to surface-layer similarity theory from 1- to 4-m temperature and wind speed differences by Hicks (1981), hereafter referred to as the Hicks method. These calculations were made from 3-h running averages of the difference measurements in order to smooth out some of the noise. An alternative to the Hicks calculations of sensible heat flux is the difference between the net radiation and the ground heat flux

($R_n - G$). Under steady-state conditions, this quantity should represent the sum of the sensible and latent heat fluxes if all other sources of heat, such as thermal advection and condensation, are negligible. If latent heat flux is also negligible, which was likely during these very dry days, $R_n - G$ can be used as an approximation of sensible heat flux. The similarity between the Hicks method for calculating sensible heat flux and $R_n - G$ for the first day supports the validity of both approaches.

In general, the modeled fluxes compare very well to the observations on both days. The magnitudes of the daily peaks and their timing are well simulated such that the peak of the sensible heat flux lags the peak in the net radiation by 1 h. Also, in both the model and the observations the sensible heat flux curves cross the net radiation curves in the afternoon at hours 7 and 31 (1600 LT). The net radiation is almost perfectly simulated on both days, which merely shows that simple radiation calculations are sufficient under such dry, clean conditions when aerosol scattering is negligible. Note that we specified the minimum surface albedo α_s for the Wangara experiment, which was 0.15 according to Edson (1980), and then computed the total surface albedo according to zenith angle as in Eq. (16).

The peak values of the model simulated sensible and ground heat fluxes are about the same on the two days, whereas the observed values differed. The measured ground heat flux was slightly higher than the modeled flux on the first day, whereas the modeled and measured values on the second day were about the same. Relative to the values computed by the Hicks method, the modeled sensible heat flux was a little low on the first day and high on the second day. However, on the second day $R_n - G$ was considerably higher than the Hicks method heat flux, which casts some doubt on the accuracy of the Hicks method estimates for this day. Note that the modeled peak value is between the Hicks method and $R_n - G$.

Figure 3 shows modeled and observed PBL heights for both days of Wangara. Observations were derived from 3-h radiosonde measurements as reported by Yamada and Mellor (1975). Only daytime PBL heights were used for this comparison so nighttime values in Fig. 3 are not meaningful for either the model or observations. The observations at hours 9 and 33 of the simulation (1800 LT) actually represent the top of the residual layer rather than active PBLs since ground-based inversions had developed by these times. We included these points, even though the actual PBL heights at these times were much lower, so that the peak of the PBL development, which probably occurred somewhere between the 1500 and the 1800 LT radiosondes, is better represented. Clearly, the model and observations compare very well in terms of the peak PBL height as well as the timing of the rise. Even the increased PBL height on the second day was accurately simulated.

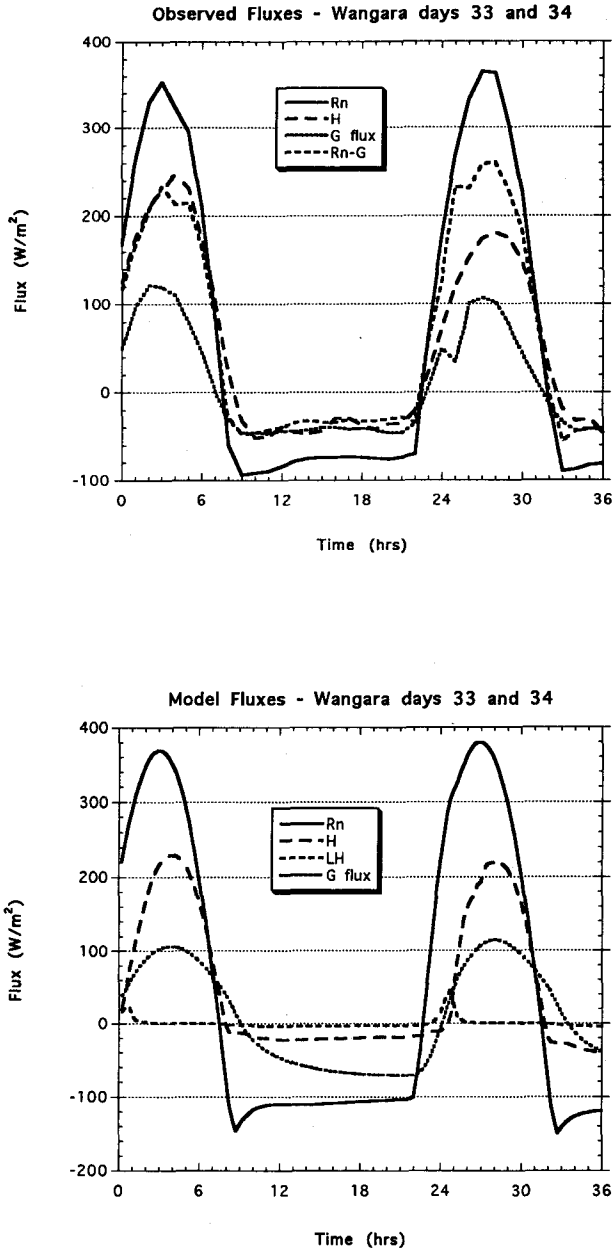

FIG. 2. Observed (top) and modeled (bottom) surface fluxes of net radiation (R_n), sensible heat (H), latent heat (LH), and ground heat (G flux) for Wangara days 33 and 34. Hour 0 is 0900 LT.

More details of the model simulations can be seen in the soundings of temperature and winds. Figure 4 shows modeled and measured vertical profiles of virtual potential temperature at four times during day 33. The 0900 sounding is the initialization so the slight differences between the two plots is just due to the interpolation of the sounding measurements to the model's vertical grid. By 1200 the surface inversion dissipated and a convective layer formed in both the modeled and measured profiles. The model, however, shows

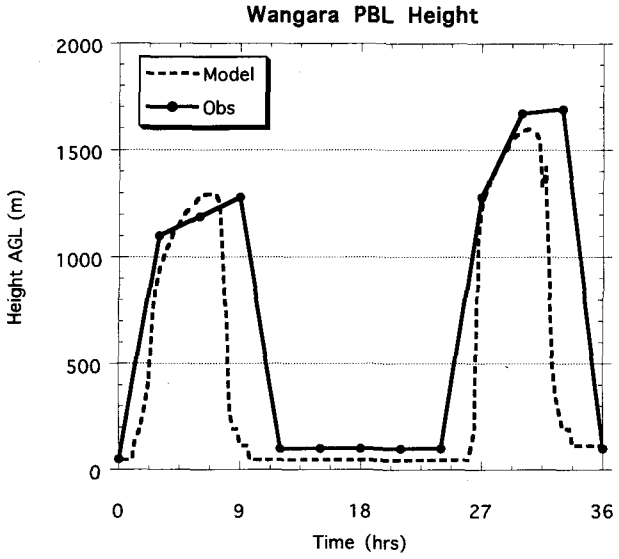

FIG. 3. Observed and modeled PBL heights for Wangara days 33 and 34.

lower temperature near the ground due to the limited vertical resolution of the model (layer 1 is about 20 m thick) compared to the measured profile, which starts with the temperature at screen height. Also, the predicted top of the convective layer is about 200 m too low. By 1500 these differences have lessened such that the height of the convective layer is about 1200 m in both the modeled and measured profiles but the lowest layer modeled temperature is still underestimated by about 1°C. The 1800 LT profiles both show a well-mixed residual layer still up to about 1200 m with a developing surface inversion. The surface temperature is now overestimated, again due to limited model resolution.

Figures 5 and 6 show modeled and measured profiles of U (eastward) and V (northward) wind components at four times during day 33 and the early morning of day 34. Again, the 0900 LT profiles are the initialization. At 1800, measurements show that the winds have become quite uniform in the PBL at moderate speeds (about 6 m s^{-1}) from the east southeast. The model simulates the U component quite well but overestimates the V component with a gradient that decreases with height. The 0300 and 0600 soundings show a well-developed nocturnal jet peaking from the east northeast at 13–14 m s^{-1} in a layer from about 200 to 400 m AGL. The modeled profiles show a nocturnal jet of similar magnitude ($\sim$12 m s^{-1}) but directed a little more from the north and more spread out vertically. Note that winds are controlled by a combination of geostrophic forcing (pressure gradient force and Coriolis force) and vertical turbulent momentum fluxes. Since the thermal winds used to define the vertical profiles of the geostrophic winds were resolved only in two 1-km-thick layers, the modeled profiles tend to have rather uniform gradients in each of the two layers.

In summary, the model performed extremely well in simulating this case from the Wangara experiment. The surface fluxes as well as the PBL height and vertical profiles of winds and temperatures compared very well with the observations. Success in this case is only a beginning, however, since the arid, clean clear sky, sparsely vegetated conditions are the simplest to model.

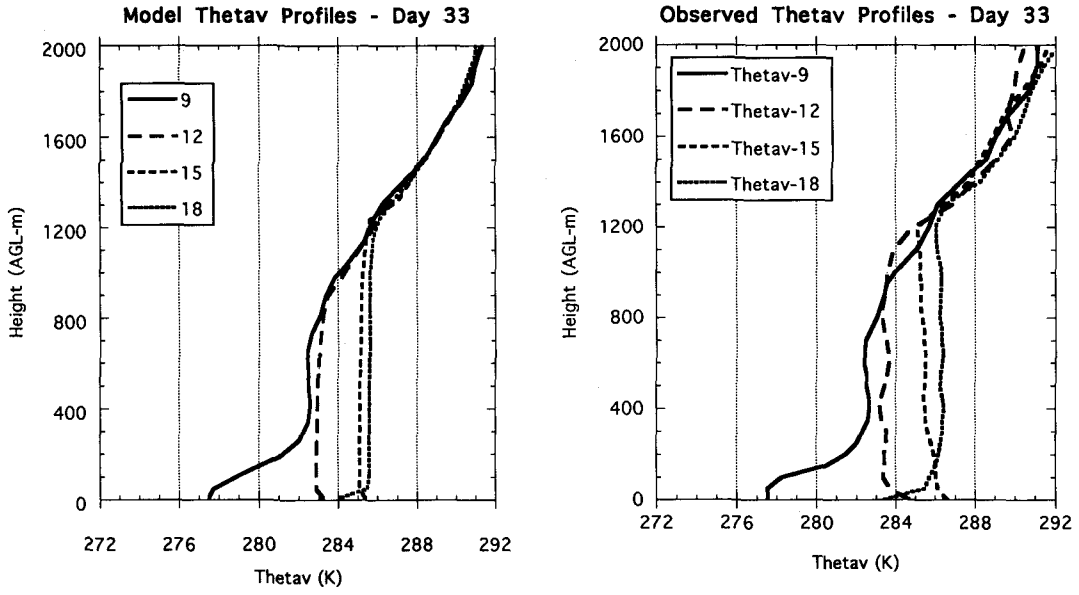

FIG. 4. Modeled (left) and measured (right) virtual potential temperature profiles at 0900, 1200, 1500, and 1800 LT on day 33.

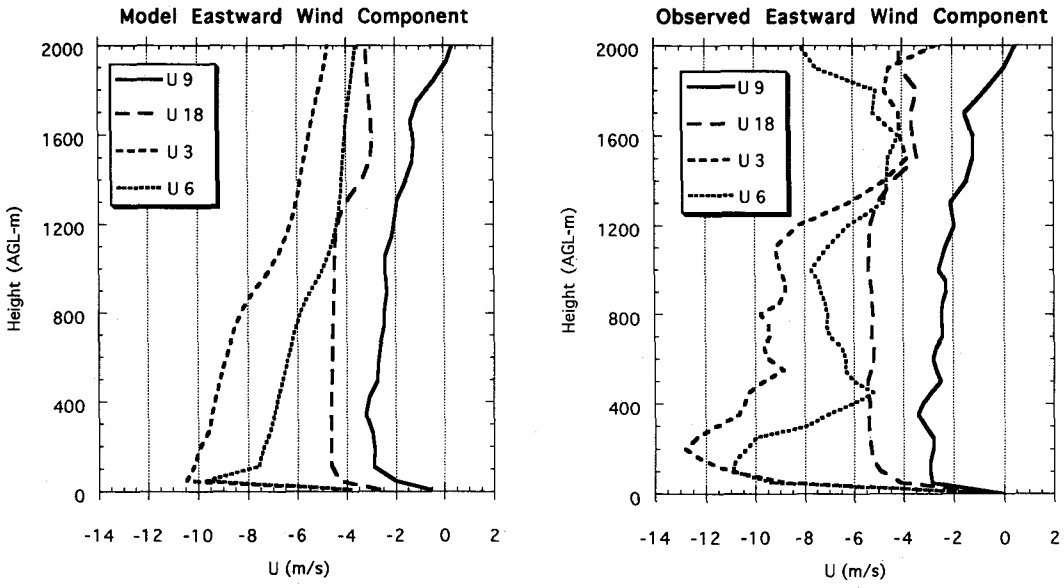

FIG. 5. Modeled (left) and measured (right) eastward wind component (U) profiles at 0900 and 1800 on day 33 and 0300 and 0600 on day 34.

Clearly, this case does not test the soil moisture, moisture flux, and vegetation-related aspects of the model. Therefore, the testing continues with two case studies from the FIFE.

b. FIFE

The second stage of model testing involves simulation of two case studies from the FIFE. The field study area was a 15 km × 15 km area of predominantly tall grass prairie near Manhattan, Kansas. An extensive monitoring program of satellite, meteorological, biophysical, and hydrological measurements was made during the growing seasons of 1987 and 1989. There were four 12–20-day intensive field campaigns (IFCs) during 1987 and one in 1989. During the IFCs, surface-based measurements were coordinated with airborne and satellite measurements (see Sellers et al. 1988, 1992a for an overview of FIFE). For this study, surface-based flux and radiosonde profile measurements were

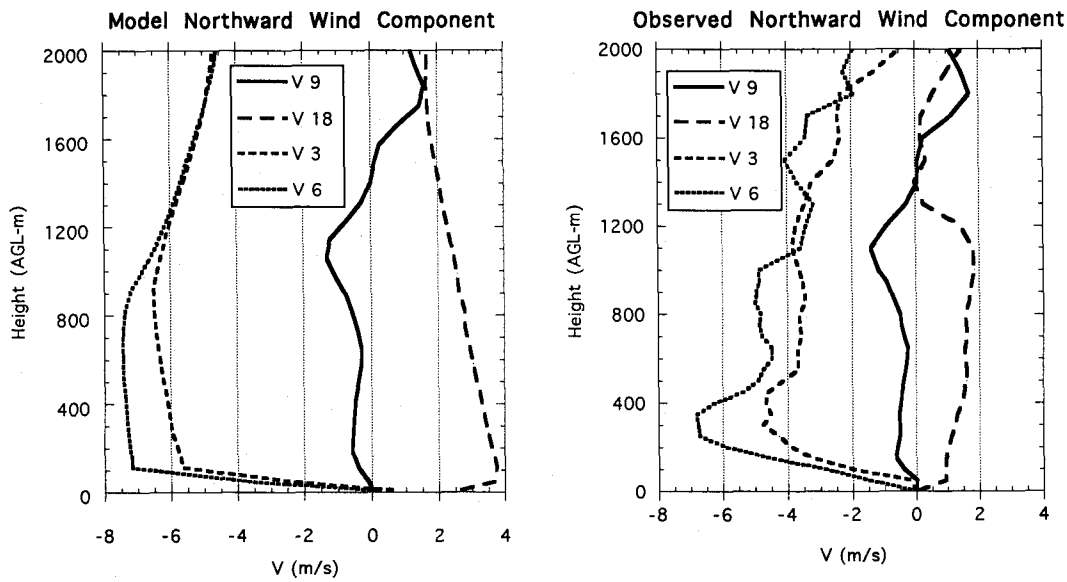

FIG. 6. Modeled (left) and measured (right) northward wind component (V) profiles at 0900 and 1800 on day 33 and 0300 and 0600 on day 34.

used for comparison to the model simulations. The experiment included measurements of sensible and latent heat fluxes made by both eddy correlation and Bowen ratio energy balance methods and ground heat flux by heat flux plates at 20 sites. In addition, there were 12 automatic meteorological stations (AMS) that measured such parameters as winds, temperature, humidity, pressure, precipitation, soil moisture, soil temperature, surface temperature, and the components of the radiation budget. Rather than averaging over all the sites in the study area we chose to model one centrally located site that included both types of flux measurements and AMS measurements. The specific site used in this study (collocated AMS site 11, eddy flux site 16, and Bowen ratio site 18) is the same one used by Kim and Verma (1990) in their study of surface energy balance and Verma et al. (1992) in their study of momentum, water vapor, and carbon dioxide exchange.

1) 11 JULY 1987

The first FIFE case study was 11 July 1987, the last day of the second IFC, which was identified as a "golden day" meaning that it was the best day of data collection for that IFC. The day was mostly clear and very windy until about 1700 CDT when significant cloud cover developed. Therefore, the model comparison breaks down at that point since the model does not yet include parameterizations for the effects of clouds. This case will be revisited when the new surface–PBL model is tested in the full 3D MM4, which includes cloud cover parameterizations. The soil moisture conditions were beginning to dry out after a very wet late June and early July. The soil at the site is predominantly Dwight silty clay loam (Kim and Verma 1990), which was modeled as silty clay loam in the USDA classification system. According to Stewart and Gay (1989) z_0 was 6.5 cm, and according to Kim and Verma (1990) and Verma et al. (1992) LAI was 2.8 at this site. The minimum surface albedo [at $Z = 0$, α_s in Eq. (16)] was set to 0.2, which is a value generally used for grassland. Surface parameters are summarized in Table 1.

The model used the same vertical grid as used for the Wangara simulation except that it was extended to 35 levels, up to almost 4 km above the ground. The profiles of wind, temperature, and humidity were initialized according to the 1200 UTC radiosonde sounding (0700 CDT). The surface soil temperature was initialized to the 1200 UTC measurement of skin temperature (22°C). The deep-layer soil temperature T_2, which represents the average temperature in the top 1 m of soil, was estimated to be 24°C from the 10-cm measurement of 24.5°C and the 50-cm temperature of 23°C. Soil moisture in the upper layer was estimated to be 27% based on the average of gravimetric measurements made at 10 sampling locations around the site at a depth of 25 mm. The deep soil moisture (1-m average) was more difficult to determine since the daily gravemetric measurements went down only to 75 mm and the neutron probe measurements, which were made at many depths down to 2 m, were infrequent such that the nearest measurements were from 8 July. The data on that day showed no significant gradient between 1 m and 20 cm with soil moisture measurements mostly from 26% to 28%. Therefore, the lower-layer soil moisture was estimated from the gravemetric measurements at 75 mm averaged over the 10 locations, which was 25.5%.

The geostrophic winds were estimated from seven radiosonde profiles during the day and were interpolated for intermediate hours. A very simple scheme was used in which only two values were input to the model. The observed winds near the top of the PBL were used to represent the geostrophic winds throughout the PBL where they are assumed to be constant with height. Likewise, the observed winds at about 2500 m were used to represent the geostrophic winds at and above this level. Between the top of the PBL and 2500 m, the geostrophic winds were linearly interpolated. Clearly, this scheme results in a far more crude estimation of the geostrophic wind profile than was used in the Wangara simulations, where a high-density spatial network of radiosondes was available.

Figure 7 shows surface fluxes measured at site 16 (eddy correlation), site 18 (Bowen ratio techniques), and model-simulated fluxes. The measurements from sites 16 and 18, which are collocated, differ only in their method of deriving the latent and sensible heat fluxes. The Bowen ratio energy balance method (BR) relies on measurements of net radiation flux and soil heat flux to define the available energy ($R_n - G$), which is then partitioned into sensible and latent heat fluxes according to the Bowen ratio. The Bowen ratio was calculated from temperature and specific humidity measurements made at two heights within the surface layer. Eddy correlation measurements (EC) were made using fast response instruments (sonic anemometers, fine wire thermocouples, and fast response optical hygrometers) to derive eddy flux covariances of heat and moisture. Each method has its pros and cons such as the assumptions of flux-profile proportionality (first-order closure of the equations of motion) and similarity ($K_H = K_E$) in the BR method. On the other hand, BR uses relatively inexpensive and simple instrumentation. Whereas the EC method is a more direct measurement of turbulent fluxes, it is more susceptible to problems in its fast response instrumentation and interference from the tower and associated structures. However, the relative agreement between the two methods supports their accuracy. Ground fluxes were derived from the average of two heat flux plates buried at a depth of 5 cm and a calculation of the soil heat storage based on the measured soil temperature for the top 5-cm soil layer. See Kanemasu et al. (1992) and Smith et al.

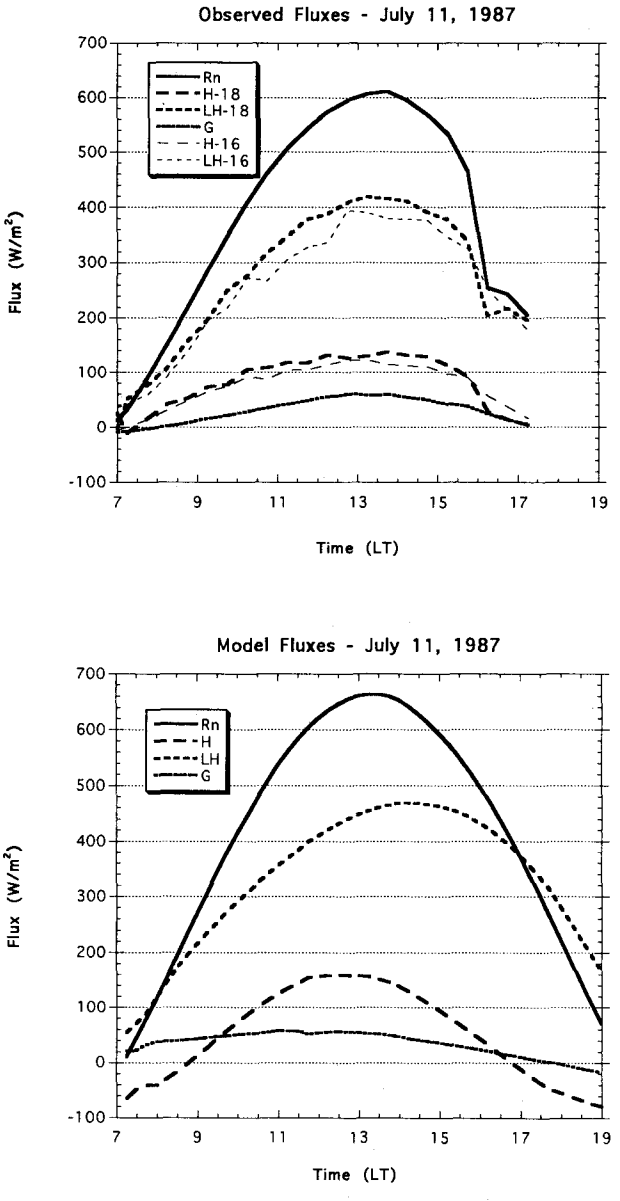

FIG. 7. Observed and modeled surface fluxes of net radiation (R_n), sensible heat (H), latent heat (LH), and ground heat (G) for 11 July 1987 of FIFE. H-18 and LH-18 were measured by Bowen ratio method, whereas H-16 and LH-16 were measured by eddy correlation.

(1992a) for detailed descriptions of the flux measurements.

The most obvious difference between the model and the measurements is that the model computed higher net radiation flux. In the late afternoon substantial cloud cover was observed, according to the FIFE cloud camera data, which obstructed much of the incoming solar radiation. However, before about 1600 LT the sky was essentially clear. Therefore, the overestimation of the peak net radiation, by about 8.5%, is due to either the underestimation of surface albedo or insufficient accounting for aerosol effects. Measurements at two sites in the FIFE study area (unfortunately not the site we modeled) showed minimum albedos of 0.15 and 0.18, which are less than the model minimum albedo of 0.20. Therefore, the overestimation of net radiation by the model may be due to underestimation of the effects of aerosols in the model, particularly at the high relative humidities observed in the PBL (87% at 1400). While the accuracy of net radiation measurements is generally estimated to be about 5%, intercomparisons reported by Smith et al. (1992a) show that midday differences between instruments were less than 10 W m^{-2}.

The peak sensible and latent heat fluxes are also overestimated compared to the observed fluxes measured by both methods. The modeled Bowen ratio, however, which is the ratio of sensible heat flux to latent heat flux, is quite similar between the model and the measurements. For example, at the peak of the net radiation curve, the modeled Bowen ratio was 0.34 while the measured Bowen ratio was 0.33 by the Bowen ratio method and 0.30 by the eddy correlation method. The peak modeled soil flux of 56 W m^{-2} compared very well to an observed peak of 59 W m^{-2}, although the model was higher than the measurements during the most of the morning. This overestimation of soil heat flux in the morning reflects a disparity in the initial turbulent fluxes, particularly sensible heat flux, between the model and the observations. This results from the combination of measurement sources used to initialize the model at 1200 UTC. Specifically, surface temperature was measured at site 18 while air temperatures were measured by a radiosonde that was released at 1143 UTC near the northern edge of the FIFE study area. Therefore, the initial air temperature in the lowest model level is not entirely consistent, either temporally or spatially, with the surface temperature. Since sensible heat flux in the model is derived from the temperature difference between the surface and the lowest model level air temperature, it is not surprising that the initial model computed sensible heat flux differs from the sensible heat flux measured at the site.

Figure 8 shows observed and modeled surface and soil temperatures. The most relevant comparison is between the observed and modeled surface temperatures T_s. The model results compare very well to the measurements as they both increase nearly linearly until about 1100 when the observed temperature starts to increase a little faster while the modeled temperature starts to curve downward. As a result, the modeled peak is about 1°C cooler than the measured peak (30°C vs 31°C). The rapid decrease in the measured surface temperature at about 1630 reflects the increasing cloudiness. The T_2 curve is the modeled deeper soil temperature that can be considered as an average of the top 1 m of soil. Measured ground temperatures at 10 cm (T_{g1}) and 50 cm (T_{g2}) are shown for compar-

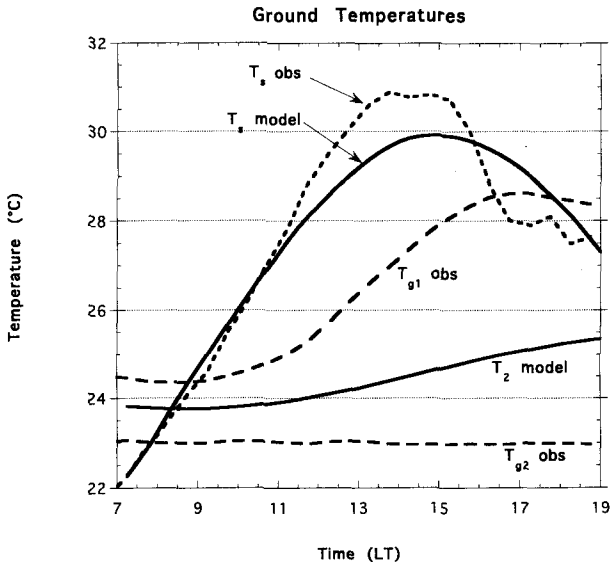

FIG. 8. Measured ground surface temperature (T_s obs), soil temperature at 10 cm (T_{g1} obs), and 50 cm (T_{g2} obs), and modeled ground surface temperature (T_s model) and average soil temperature in top 1 m (T_2 model) for 11 July 1987 of FIFE.

ison. The T_2 curve fits nicely between the two observed curves.

One of the main reasons for developing this model is to improve the PBL height simulations in MM4, which are so crucial to air quality modeling. Figure 9 shows the modeled PBL heights compared to estimates of the PBL height derived from six radiosondes. Both the modeled and observed PBL heights were estimated by the bulk Richardson number method [Eq. (6)]. The model was initialized with the 1200 UTC sounding. The model compares quite well at the PBL maximum in the afternoon. However, during the time of most rapid PBL development, the model lags the observations by almost 2 h. A possible reason for this discrepancy is the model's inability to sufficiently account for both shear induced turbulence and buoyancy induced turbulence at the same time. As described above, the PBL model is a hybrid of a PBL scaling eddy diffusivity model and a nonlocal closure-free convective model (ACM). Usually during clear summer days, buoyancy dominates PBL turbulence and the ACM performs quite well. However, this case was very windy (about 15–20 m s^{-1} in the PBL), such that shear turbulence was also very important. In fact, h/L was about -2 for much of the day, which indicates that buoyancy and shear were equally important at $z = h/2$. Therefore, neither the ACM, which includes no shear effects, nor the eddy diffusion model, which cannot adequately simulate convective transport, are sufficient for this case. This suggests the need for more generalized transilient models of the type developed by Stull and Driedonks (1987). The challenge is to develop a model that is sufficiently general and simple enough to run quickly in 3D Eulerian grid models.

2) 6 JUNE 1987

The second case study from the FIFE was 6 June 1987, which was the last day of IFC 1 and also a "golden day." The sky was completely clear of clouds for the whole day and the winds were more moderate than the previous case at about 10–12 m s^{-1} from the south in the PBL. Since it was earlier in the growing season, the LAI was 1.9 (Verma et al. 1992) and z_0 was about 4.5 cm (Sellers et al. 1992b). Soil moisture conditions were again rather moderate after three days of clear weather during which time the soil was drying from near-saturated conditions the previous week.

The model profiles of winds, temperature, and humidity were initialized to the 1200 UTC (0700 CDT) sounding. The surface and lower-layer soil temperatures were initialized to the 1200 UTC measurements, which were 16.0°C and 20.2°C, respectively. The initial soil moisture for the top 1 cm was set to 23%, which is just slightly less than the 10 sample average of gravemetric measurements at a depth of 25 mm, which was 24.3%. Since this day was in the midst of a drying trend, the shallower 1-cm model layer should be a little dryer than the deeper measurements. The initial moisture in the 1-m model soil layer was again more difficult to estimate. The average of the gravemetric measurements at 75 mm was 26% and the neutron probe data from 3 June show a slight decreasing gradient with depth in the top 1-m layer. Therefore, 25% was used as the initial soil moisture for the deeper (1 m) model layer.

Figure 10 shows surface fluxes measured at site 18 (BR) and computed by the model. Eddy correlation

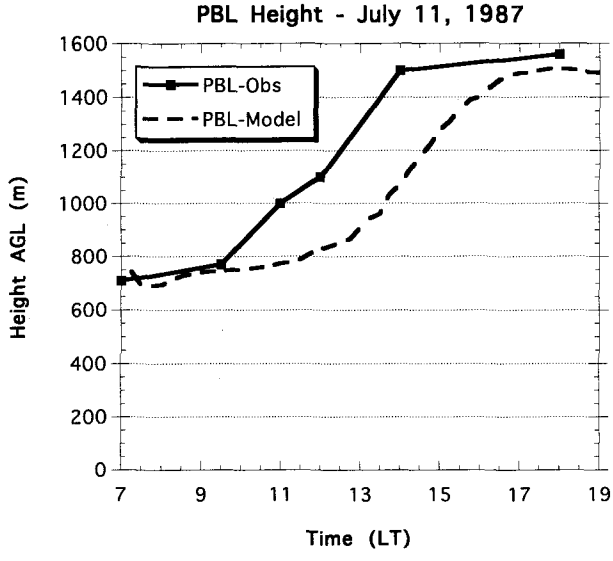

FIG. 9. Observed and modeled PBL heights for 11 July 1987 of FIFE.

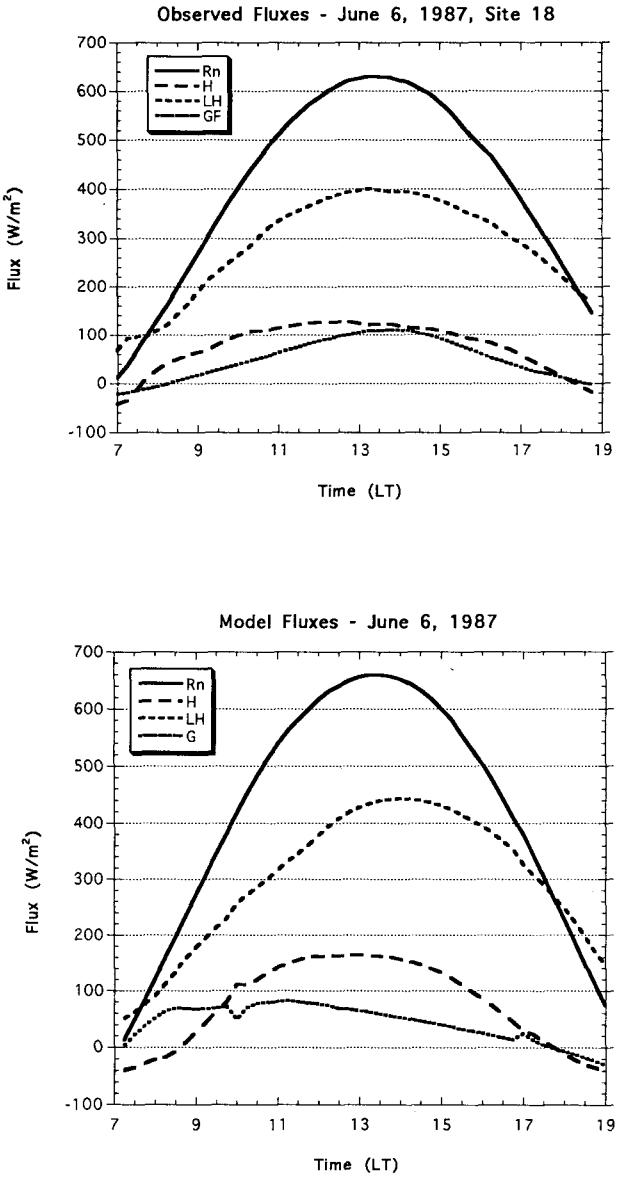

FIG. 10. Observed and modeled surface fluxes of net radiation (R_n), sensible heat (H), latent heat (LH), and ground heat (G) for 6 June 1987 of FIFE.

measurements were not available for this day. The model again overestimates the maximum net radiation at the surface compared to the measurements but by a lesser degree than for the 11 July case. The reason for the better radiation simulation (about 5% difference at the peak) for this case may be the clearer skies and lower humidity in the PBL. The peak values of the latent heat and sensible heat fluxes are also overestimated by the model by a somewhat greater degree than the net radiation. The greater amount of energy available for the turbulent surface fluxes results from a combination of the overprediction of net radiation and underprediction of ground heat flux. The peak modeled ground heat flux was 82 W m^{-2}, whereas the peak measured ground heat flux was 110 W m^{-2}. In the early afternoon (1300–1400) the underprediction was even greater since the modeled ground heat flux peaked earlier in the day (around 1100) than the measured ground heat flux. The Bowen ratio of the model results at peak net radiation is slightly higher (0.37) than the observations (0.32). The model, however, is very sensitive to the initial specification of the deep-layer soil moisture, which is not well known. For example, changing the initialization from 25% to 26% changes the Bowen ratio from 0.37 to 0.30.

The kinks in the modeled sensible heat flux and ground heat flux curves (Fig. 10) at 1000 and again at about 1700 are caused by the transition from the eddy diffusion model to the convective model (ACM) in the morning and then back to the eddy diffusion model in the afternoon. These transitions cause slight oscillations in the surface temperatures and heat fluxes that very quickly damp out.

Time series of modeled and measured soil temperatures (shown in Fig. 11) indicate that the model significantly underestimates surface temperature throughout the middle of the day. For the first two hours of the simulation (0700–0900), the model and the measurements compare quite well and again for the last two hours (1700–1900). However, in between the measurements peak almost 4.5°C higher than the model. Underprediction of surface temperature could result from too large surface heat capacity in the model. Recall that our modification of the Noilhan and Planton (1989) model effectively increased the bulk surface heat capacity to be more like the value for soil. There-

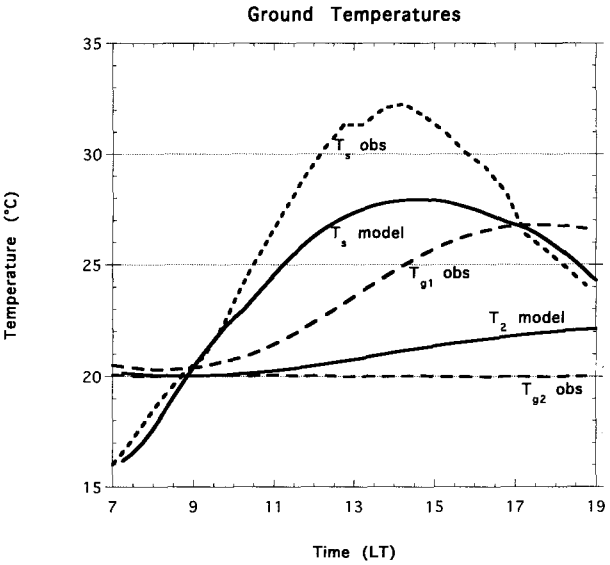

FIG. 11. Measured ground surface temperature (T_s obs), soil temperature at 10 cm (T_{g1} obs), and 50 cm (T_{g2} obs), and modeled ground surface temperature (T_s model) and average soil temperature in top 1 m (T_2 model) for 6 June 1987 of FIFE.

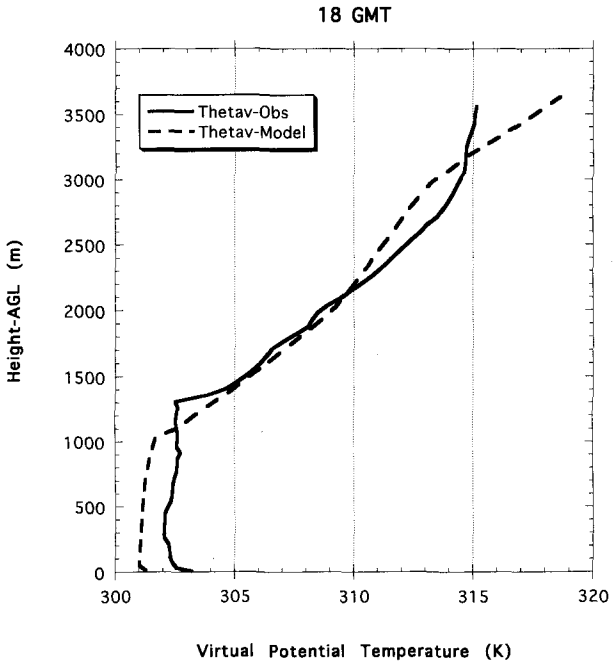

FIG. 12. Modeled and measured virtual potential temperature profiles at 1800 UTC (1300 LT) 6 June 1987.

fore, we tested the effect of this modification by rerunning the model with a much smaller heat capacity (by about two orders of magnitude). The result was an increase in peak surface temperature of less than 1°C and a decrease of the soil heat flux to a peak of about 1 W m^{-2}. Clearly, the discrepancy in the surface temperature was not due to heat capacity.

The underprediction of soil flux is consistent with the underprediction of surface temperature because of the smaller temperature gradient between the surface and deeper soil. Also, the underprediction of soil flux results in the underprediction of surface temperature since less energy in available for heating the soil. The underprediction of surface temperature, however, is not consistent with the overprediction of sensible heat flux. In the absence of unaccounted for heat sources in the PBL the model's lower surface temperature should lead to a lesser temperature gradient between the surface and the air and hence smaller sensible heat flux. Therefore, the overprediction of sensible heat flux suggests that the air temperature was also underpredicted. Comparison of virtual potential temperature profiles at 1300 (Fig. 12) show that the modeled air temperature in the PBL is indeed less than observed. The only conclusion that fits these facts is that the air in the PBL was heated by some process missing from the model formulation, most probably warm advection on the predominantly southerly winds. Warm advection in the PBL is not simulated by the 1D model, which therefore underestimates the temperature and height of the PBL and therefore also the surface temperature and soil flux.

The comparison of observed and modeled PBL heights (Fig. 13) also indicates the possibility of warm advection since the model underestimates the observed PBL heights at all times after the initialization. The virtual potential temperature profiles at 1800 UTC (1300 LT), shown in Fig. 12, demonstrate that the shallower mixed layer in the model is associated with cooler PBL temperatures (by about 1°C). The similarity between the observed and predicted profiles above the PBL indicates that significant thermal advection was not occurring at these levels.

c. Sensitivity to soil moisture

The sensitivity of PBL height and surface temperature, which are critically important parameters for air quality simulation, to variations in soil moisture is tested. The 6 June 1987 FIFE case is used to illustrate how the simulation would change when only the initial soil moisture is varied from wilting point to field capacity. Figures 14 and 15 show the PBL heights and surface temperatures resulting from three simulations: 1) the FIFE simulation as described above with initial w_g = 23% and w_2 = 25%; 2) the initial soil moisture set to field capacity ($w_g = w_2$ = 32.2%); and 3) the initial soil moisture set to wilting point ($w_g = w_2$ = 21.8%). Note that the entire range from wilting point to field capacity is only about 10% for silty clay loam. Furthermore, the difference between the FIFE initialization and the wilting point is only about 3%, which is less than the typical standard deviation of soil moisture (σ_θ) for field sizes on the order of 0.1 km^2 (Wetzel and Chang 1988). This small change in soil moisture,

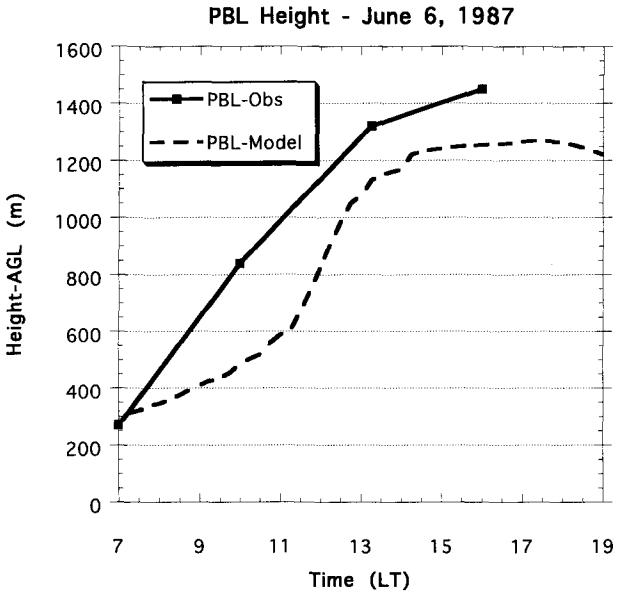

FIG. 13. Observed and modeled PBL heights for 6 June 1987 of FIFE.

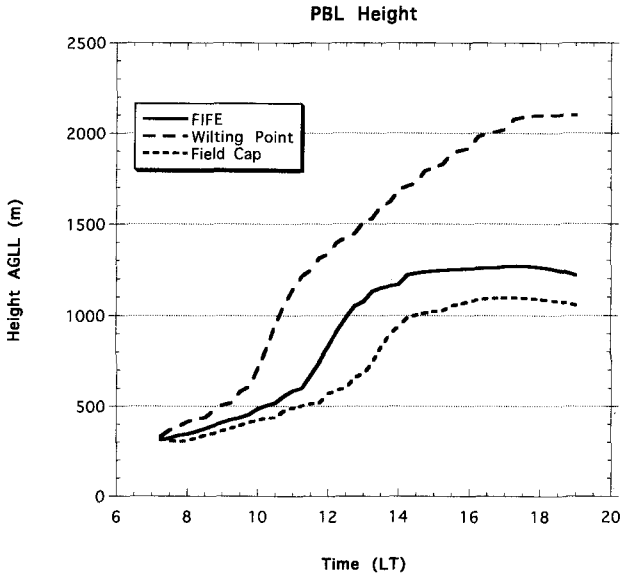

FIG. 14. Sensitivity of modeled PBL heights to initial soil moisture for 6 June 1987 of FIFE.

however, results in a huge change in PBL height, from a maximum for the FIFE initialization of 1270 to 2100 m for the wilting point run (Fig. 14). Similarly, Fig. 15 shows that the maximum surface temperature for the wilting point simulation is 8.5°C higher than for the FIFE initialization. The differences between the FIFE initialization and the field capacity run are much smaller even though the change in initial soil moisture was greater. This exercise demonstrates that a model that is insensitive to soil moisture conditions is prone to significant errors in PBL and surface temperature simulations.

The dramatic effect of changing the initial soil moisture to the wilting point is due to the complete cessation of evapotranspiration. The model parameterizes stomatal conductance as a linear function of root zone soil moisture w_2 between wilting point and field capacity. This effect is so extreme because of the almost complete coverage of the ground by vegetation in the FIFE study area. Note that the model drastically simplifies the situation, particularly by neglecting the high degree of spatial variation inherent in soil moisture. In reality, there is always a distribution of soil moisture even over very small spatial scales. For example, Wetzel and Chang (1988) estimate $\sigma_\theta \sim 7\%$ for grid sizes on the order of 100 km^2. Therefore, when the average soil moisture is near wilting point some parts of the distribution dip below wilting point, whereas other parts remain above wilting point enabling some evapotranspiration to continue. Consequently, spatial averaging of soil moisture, as in Eulerian grid models, can lead to significant errors, particularly near wilting point or field capacity. Wetzel and Chang (1988) have developed a scheme that uses subgrid distributions of soil moisture thus allowing evapotranspiration to occur at different degrees of water stress in the same grid cell. We plan to include a similar scheme for subgrid heterogeneity as part of our MM4 modifications.

4. Summary and conclusions

Initial tests of the model in 1D form are compared to field studies from Wangara in Australia (dry, sparse vegetation) and FIFE in northeast Kansas (moist tall grass prairie). Preliminary results from the simulation of days 33 and 34 of the Wangara experiment show very good agreement with observations of surface fluxes, PBL height, and profiles of temperature and winds. Whereas the Wangara simulation provided a good test case for the PBL model and the flux profile algorithms, it did little to test the soil moisture model and the partitioning of sensible and latent heat fluxes since the site was so arid. Therefore, two cases from the FIFE are also studied so that the vegetation and soil moisture components of the model could be tested. The FIFE simulations show that the model tends to overestimate net radiation when humidity is high, suggesting that aerosol scattering may be underpredicted. The model also overestimated sensible and latent heat fluxes by a small amount in both cases. The ground flux predictions were quite close to the measurements in the 11 July case but underpredicted in the 6 June case. Surface temperature was slightly underpredicted in the 11 July case and greatly underpredicted in the 6 June case, which was probably due to warm advection.

The most positive result of the FIFE simulations was the good agreement between the modeled and ob-

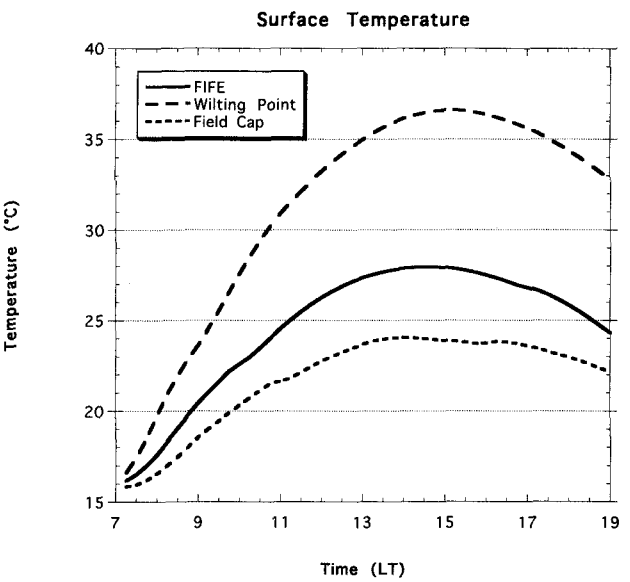

FIG. 15. Sensitivity of modeled surface temperature to initial soil moisture for 6 June 1987 of FIFE.

served Bowen ratios. This shows that the model is capable of realistic simulation of moisture fluxes primarily by transpiration through vegetation. Also, the maximum PBL height simulation for 11 July was quite close to the observation even though the rise was too slow. The slow rise of the PBL could be an indication that the PBL model cannot adequately simulate PBL mixing and growth on very windy but clear days when both buoyancy and shear-induced turbulence are important. In addition, part of the difficulty in trying to simulate surface fluxes and PBL processes in a coupled fashion may be that the surface fluxes are responding to turbulence induced by vegetative roughness, while the PBL turbulence may be more associated with terrain.

In general, the simulation of 11 July was better than the 6 June case. The main reason for this is probably that horizontal warm advection was occurring in the PBL during the middle of the day on 6 June. We are planning to revisit both of these cases with the 3D MM4 modified to include this new surface–PBL model. With the 3D model we should be able to see if warm advection was indeed an important factor on 6 June.

The sensitivity tests of PBL height and surface temperature to soil moisture demonstrates the importance of the realistic simulation and initialization of soil moisture in meteorological models. These tests also suggest the need for representation of soil moisture subgrid heterogeneity in Eulerian grid models. Using grid cell averages of soil moisture tends to exaggerate the effects of extreme conditions, near wilting point or field capacity. Therefore, some scheme for the representation of subgrid heterogeneity will be applied to the MM4 modifications.

The FIFE database contains an enormous wealth of information that will be very valuable for continuing the development of surface–PBL modeling techniques for mesoscale modeling. For example, the extensive radiation measurements will help construct and improve radiation algorithms for both clear and cloudy skies. Also, the variety of flux measurements from the surface sites and aircraft may help resolve some of the issues related to the scale of roughness appropriate for grid cell average calculations as well as the influence of subgrid heterogeneity.

The next phase of this work, which has already begun, is to incorporate the surface–PBL model discussed here into the MM4–MM5 system. The modified MM4 results will be extensively compared to the current model values and also to field study data. The key features of this model, which represent a significant advance over the current model in the MM4–MM5 system, are the prognostic simulation of soil moisture and the parameterization of vegetative evapotranspiration. This allows the model to be more responsive to changing moisture conditions due to precipitation and evaporation, thereby enabling a better simulation of the partitioning of surface energy into latent and sensible heat flux components. As a result, the simulation of the evolution of PBL heights, which are extremely important to air pollutant concentration simulations, and surface temperatures, which are key factors determining biogenic emissions, should be significantly improved.

The incorporation of this model into the MM4–MM5 system requires additional data inputs as well as modifications to the initialization and 4D data assimilation techniques. The additional data includes soil texture type and some additional land use parameters such as leaf area index and fractional vegetation coverage. High resolution ($\sim$1 km) datasets for both soil and land use parameters are currently under development and should be available for this work.

Disclaimer. The information in this document has been funded wholly or in part by the United States Environmental Protection Agency. It has been subjected to agency review and approved for publication. Mention of trade names or commercial products does not constitute endorsement or recommendation for use.

Acknowledgements. The authors appreciate the work accomplished by the entire FIFE team and particularly the FIFE Information System (FIS) staff, headed by Don Strebel, for making this remarkable dataset so easily accessible.

REFERENCES

André, J. C., J. P. Goutorbe, and A. Perrier, 1986: HAPEX–MOBILHY: A hydrologic atmospheric experiment for the study of water budget and evaporation flux at the climatic scale. *Bull. Amer. Meteor. Soc.*, **67,** 138–144.

Anthes, R. A., E.-Y. Hsie, and Y.-H. Kuo, 1987: Description of the Penn State/NCAR Mesoscale Model Version 4 (MM4). NCAR Tech. Note, NCAR/TN-282+STR, 66 pp.

Argentini, S., P. J. Wetzel, and V. M. Karyampudi, 1992: Testing a detailed biophysical parameterization for land–air exchange in a high-resolution boundary-layer model. *J. Appl. Meteor.*, **31,** 142–156.

Avissar, R., and R. Pielke, 1989: A parameterization of heterogeneous land surfaces for atmospheric numerical models and its impact on regional meteorology. *Mon. Wea. Rev.*, **117,** 2113–2136.

Binkowski, F. S., 1983: A simple model for the diurnal variation of the mixing depth and transport flow. *Bound.-Layer Meteor.*, **27,** 217–236.

Blackadar, A. K., 1976: Modeling the nocturnal boundary layer. *Third Symp. on Atmospheric Turbulence, Diffusion and Air Quality,* Raleigh, NC, Amer. Meteor. Soc., 46–49.

——, 1978: Modeling pollutant transfer during daytime convection, Preprints, *Fourth Symp. on Atmospheric Turbulence, Diffusion, and Air Quality,* Reno, NV, Amer. Meteor. Soc., 443–447.

Bougeault, P., J. Noilhan, P. Lacarrère, and P. Mascart, 1991a: An experiment with an advanced surface parameterization in a mesobeta-scale model. Part I: Implementation. *Mon. Wea. Rev.*, **119,** 2358–2373.

——, B. Bret, P. Lacarrère, and J. Noilhan, 1991b: An experiment with an advanced surface parameterization in a mesobeta-scale model. Part II: The 16 June 1986 simulation. *Mon. Wea. Rev.*, **119,** 2374–2392.

Byun, D. W., 1990: On the analytical solutions of flux-profile relationships for the atmospheric surface layer. *J. Appl. Meteor.*, **29,** 652–657.

——, 1991: Determination of similarity functions of the resistance laws for the planetary boundary layer using surface-layer similarity functions. *Bound.-Layer Meteor.*, **57,** 17–48.

Carlson, T. N., and F. E. Boland, 1978: Analysis of urban–rural canopy using surface heat flux/temperature model. *J. Appl. Meteor.*, **17,** 998–1013.

Chang, J. S., R. A. Brost, I. S. A. Isaksen, S. Madronich, P. Middleton, W. R. Stockwell, and C. J. Walcek, 1987: A three-dimensional Eulerian acid deposition model: Physical concepts and formulation. *J. Geophys. Res.*, **92,** 14 681–14 700.

Clapp, R. B., and G. M. Hornberger, 1978: Empirical equations for some soil hydraulic properties. *Water Resour. Res.*, **14,** 601–604.

Clarke, R. H., A. J. Dyer, R. R. Brook, D. G. Reid, and A. J. Troup, 1971: The Wangara experiment: Boundary layer data. Tech. Paper No. 19, CSIRO, Division of Meteorological Physics, Aspendale, Australia, 362 pp.

Deardorff, J., 1974: Three-dimensional numerical study of the height and mean structure of a heated planetary boundary layer. *Bound.-Layer Meteor.*, **7,** 81–106.

——, 1978: Efficient prediction of ground surface temperature and moisture, with inclusion of a layer of vegetation. *J. Geophys. Res.*, **83,** 1889–1903.

Dickinson, R. E., A. Henderson-Sellers, P. J. Kennedy, and M. F. Wilson, 1986: Biosphere–atmosphere transfer scheme (BATS) for the NCAR Community Climate Model. NCAR Tech. Note, NCAR/TN-275+STR, 69 pp.

Edson, R. T., 1980: Parameterization of net radiation at the surface using data from the Wangara experiment. Environmental Research Papers, Colorado State University, Fort Collins, CO, 26 pp.

Hicks, B. B., 1981: An analysis of Wangara micrometeorology: Surface stress, sensible heat, evaporation, and dewfall. NOAA Tech. Memo. ERL-104, 36 pp.

Holtslag, A. A. A., and F. T. M. Nieuwstadt, 1986: Scaling the atmospheric boundary layer. *Bound.-Layer Meteorol.*, **36,** 201–209.

——, E. I. F. de Bruijn, and H.-L. Pan, 1990: A high resolution air mass transformation model for short-range weather forecasting. *Mon. Wea. Rev.*, **118,** 1561–1575.

Idso, S., R. Jackson, B. Kimball, and F. Nakayama, 1975: The dependence of bare soil albedo on soil water content. *J. Appl. Meteor.*, **14,** 109–113.

Jacquemin, B., and J. Noilhan, 1990: Sensitivity study and validation of a land surface parameterization using the HAPEX–MOBILHY data set. *Bound.-Layer Meteor.*, **52,** 93–134.

Kanemasu, E. T., S. B. Verma, E. A. Smith, L. J. Fritschen, M. Wesely, R. T. Field, W. P. Kustas, H. Weaver, J. B. Stewart, R. Gurney, G. Panin, and J. B. Moncrieff, 1992: Surface flux measurements in FIFE: An overview. *J. Geophys. Res.*, **97,** 18 547–18 555.

Kim, J., and S. B. Verma, 1990: Components of surface energy balance in a temperate grassland ecosystem. *Bound.-Layer Meteor.*, **51,** 401–417.

McCumber, M. C., and R. A. Pielke, 1981: Simulation of the effects of surface fluxes of heat and moisture in a mesoscale numerical model. Part I: Soil layer. *J. Geophys. Res.*, **86,** 9929–9938.

Mihailovic, D. T., H. A. R. de Bruin, M. Jeftic, and A. van Dijken, 1992: A study of the sensitivity of land surface parameterizations to the inclusion of different fractional covers and soil textures. *J. Appl. Meteor.*, **31,** 1477–1487.

Monteith, J. L., 1961: An empirical method for estimating long wave radiation exchanges in the British Isles. *Quart. J. Roy. Meteor. Soc.*, **87,** 171–179.

Noilhan, J., and S. Planton, 1989: A simple parameterization of land surface processes for meteorological models. *Mon. Wea. Rev.*, **117,** 536–549.

——, P. Lacarrère, and P. Bougeault, 1991: An experiment with an advanced surface parameterization in a mesobeta-scale model. Part III: Comparison with the HAPEX–MOBILHY dataset. *Mon. Wea. Rev.*, **119,** 2393–2413.

Paltridge, G. W., and C. M. R. Platt, 1976: *Radiative Processes in Meteorology and Climatology.* Elsevier, 57–63.

Pielke, R. A., G. A. Dalu, J. S. Snook, T. J. Lee, and T. G. F. Kittel, 1991: Nonlinear influence of mesoscale land use on weather and climate. *J. Climate,* **4,** 1053–1069.

Pleim, J. E., and J. S. Chang, 1992: A non-local closure model for vertical mixing in the convective boundary layer. *Atmos. Environ.*, **26A,** 965–981.

——, and J. K. S. Ching, 1993: Interpretive analysis of observed and modeled mesoscale ozone photochemistry in areas with numerous point sources. *Atmos. Environ.*, **27A,** 999–1017.

Sellers, P. J., Y. Mintz, Y. C. Sud, and A. Dalcher, 1986: A simple biosphere model (SiB) for use within general circulation models. *J. Atmos. Sci.*, **43,** 505–531.

——, F. G. Hall, G. Asrar, D. E. Strebel, and R. E. Murphy, 1988: The First ISLSCP Field Experiment (FIFE). *Bull. Amer. Meteor. Soc.*, **69,** 22–27.

——, ——, ——, ——, and ——, 1992a: An overview of the First International Satellite Land Surface Climatology Project (ISLSCP) Field Experiment (FIFE). *J. Geophys. Res.*, **97,** 18 345–18 371.

——, M. D. Heiser, and F. G. Hall, 1992b: Relations between surface conductance and spectral vegetation indices at intermediate (100 m^2 to 15 km^2) length scales. *J. Geophys. Res.*, **97,** 19 033–19 059.

Smith, E. A., W. L. Crosson, and B. D. Tanner, 1992a: Estimation of surface heat and moisture fluxes over a prairie grassland. 1: In situ energy budget measurements incorporating a cooled mirror dew point hygrometer. *J. Geophys. Res.*, **97,** 18 557–18 582.

——, A. Y. Hsu, W. L. Crosson, R. T. Field, L. J. Fritschen, R. J. Gurney, E. T. Kanemasu, W. P. Kustas, D. Nie, W. J. Shuttleworth, J. B. Stewart, S. B. Verma, H. L. Weaver, and M. L. Wesely, 1992b: Area-averaged surface fluxes and their time–space variability over the FIFE experimental domain. *J. Geophys. Res.*, **97,** 18 599–18 622.

Stewart, J. B., and L. W. Gay, 1989: Preliminary modeling of transpiration from the FIFE site in Kansas. *Agric. For. Meteor.*, **48,** 305–315.

Stull, R. B., and A. G. M. Driedonks, 1987: Applications of the transilient turbulence parameterization to atmospheric boundary-layer simulations. *Bound.-Layer Meteor.*, **40,** 209–239.

Troen, I., and L. Mahrt, 1986: A simple model of the atmospheric boundary layer; sensitivity to surface evaporation. *Bound.-Layer Meteor.*, **37,** 129–148.

Verma, S. B., J. Kim, and R. J. Clement, 1992: Momentum, water vapor, and carbon dioxide exchange at a centrally located prairie site during FIFE. *J. Geophys. Res.*, **97,** 18 629–18 639.

Wetzel, P. J., and J.-T. Chang, 1987: Concerning the relationship between evapotranspiration and soil moisture. *J. Climate Appl. Meteor.*, **26,** 18–27.

——, and ——, 1988: Evapotranspiration from nonuniform surfaces: A first approach for short-term numerical weather prediction. *Mon. Wea. Rev.*, **116,** 600–621.

——, and S. Argentini, 1990: The sensitivity of daytime low cloud amount to vegetation cover, soil moisture and pre-dawn sounding—Two case studies. Preprints, *Eighth Conf. on Hydrometeorology,* Kananaskis Park, Canada, Amer. Meteor. Soc., 12–17.

Wilson, M. F., A. Henderson-Sellers, R. E. Dickinson, and P. J. Kennedy, 1987: Sensitivity of the Biosphere–Atmospheric Transfer Scheme (BATS) to the inclusion of variable soil characteristics. *J. Climate Appl. Meteor.*, **26,** 341–362.

Wyngaard, J. C., and O. R. Coté, 1974: The evolution of a convective boundary layer—A higher-order-closure model study. *Bound.-Layer Meteor.*, **7,** 289–308.

Yamada, T., and G. Mellor, 1975: A simulation of the Wangara atmospheric boundary layer data. *J. Atmos. Sci.*, **32,** 2309–2329.